ILASS–Europe 2022, 31th Conference on Liquid Atomization and Spray Systems, 6-8 September 2022, Virtual, Israel

Characteristics of Multiple Droplet Impacts on Solid Surfaces

Anjan Goswami*, Yannis Hardalupas
Mechanical Engineering Department, Imperial College London, London SW7 2AZ, UK
*Corresponding author: a.goswami19@imperial.ac.uk

Abstract
The simultaneous or non-simultaneous impact of two droplets on solid surface can lead to multiple lamella interactions that generate an uprising central sheet, which may break into droplets or fall back on the impact surface. A micro-controller-based droplet generator was developed that releases two equal-sized droplets on demand, simultaneously or not. For a given inter-droplet spacing and impact Weber number, the temporal evolution of the central sheet is investigated for different time lags between impacts. For simultaneous impacts (no time lag), the uprising sheet evolves vertically as a two-dimensional (2D) 'semilunar' shape with linear sheet base. For non-simultaneous impacts, the morphology of the sheet evolution depends on time lag, varying from inclined 2D 'semilunar' sheet with linear base to 3D sheet with curved base. The effect of time lag between impacts on the central sheet position, height, width and inclination is quantified, providing new insights on multiple droplet impact dynamics.

Keywords
Droplet generator, Simultaneous and Non-simultaneous droplet Impacts, Central sheet

Introduction

The impact of liquid droplets onto solid surfaces is ubiquitous in nature, medical, agricultural, and industrial applications, including falling raindrops, sneezing, cryogenic tissue cooling, pesticide spraying, surface coating, spray cooling, etc. The impact of a single droplet on surfaces has been studied widely to date to understand and control the pertinent outcomes, e.g. see [1,2] for comprehensive reviews. On the other hand, multiple droplet impact on surfaces is far less investigated, despite its greater prevalence in practical applications.

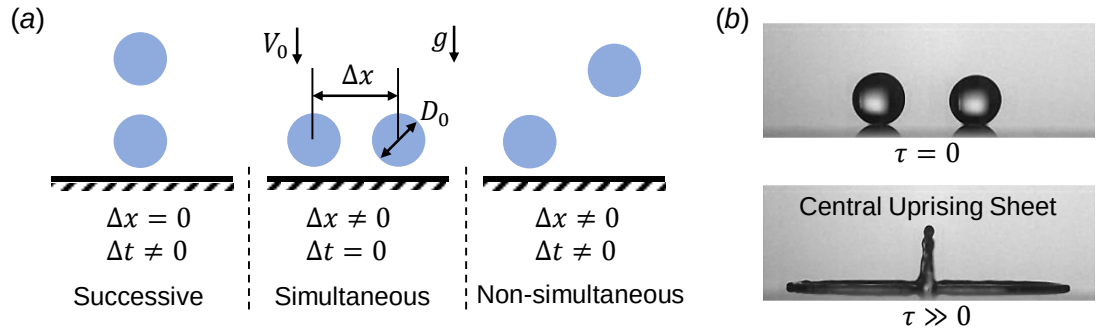

Figure 1. (a) Multiple droplet impact scenarios with spatial and temporal criteria. (b) Images of droplets touchdown on a surface (at $\tau = 0$) and of the central uprising sheet (at $\tau \gg 0$) formed during the simultaneous impact of droplets.

Droplet impact processes are usually characterised by dimensionless Weber number, $We = \rho D_0 V_0^2/\sigma$, where ρ, D_0, V_0, and σ represent the liquid density, initial droplet diameter, impact velocity and surface tension respectively. The temporal evolution of impact processes is characterised by a dimensionless time $\tau = tV_0/D_0$, where t is the dimensional time. Based on the inter-droplet spacing (Δx) and the time lag (Δt) between impacts, multiple droplet

impacts can be successive, simultaneous, and non-simultaneous (**Figure 1(a)**). Among these three cases, the case of successive impacts is more investigated than the latter two cases [3]. For simultaneous and non-simultaneous impacts ($\Delta x \neq 0$) with high impact velocity, the interaction of the two spreading droplets on the surface leads to the formation of a central uprising sheet (**Figure 1(b)**), which modifies the outcome of equivalent single droplet impacts. For instance, this central sheet can become unstable, leading to a lower splashing threshold [4] and generation of larger droplets [5] than for an equivalent single droplet impact process. Roisman et al. [6] experimentally demonstrated that the uprising sheet remains vertical for simultaneous impacts, whereas it inclines towards the earlier droplet for non-simultaneous impacts. The authors reported a theoretical model to estimate the maximum central sheet height (H_{CS}) for simultaneous impacts. Gultekin et al. [7] investigated the effect of inter-droplet spacing and impact Weber number on the central sheet height (H_{CS}) for simultaneous impacts. Liang et al. [8] explored the time-resolved evolution of the central sheet with a single side view of the sheet. However, simultaneous imaging of the sheet evolution from different views is important to detail the central sheet morphologies. Ersoy et al. [9] showed that the central sheet initially evolves with a 'semilunar' shape during its vertical ascent and instability cusps may appear at the sheet rim at later stages. A characterisation of the central sheet evolution based on the time lag between droplet impacts is missing from the literature.

This study quantifies the effect of the time lag between impacts on the temporal evolution of the central sheet, investigating the impact processes simultaneously from different views. The next section describes the experimental setup and the droplet generator. The following section presents results for different conditions and initially shows the characteristics of the impact using simultaneous images from two views at different times. Then it reports quantitative information on the temporal evolution of the central liquid sheet height and its position on the impacting surface and its inclination angle. The paper ends with a summary of the main conclusions.

Experimental Arrangement and Methodology

Figure 2 shows a simplified schematic of the experimental arrangement. An in-house built on-demand generator of two identical droplets is based on a syringe pump connected to a customised needle assembly. The pump was developed using a microcontroller-based (Arduino with motor shield) system to precisely actuate a fine stepper motor to deliver a certain amount of liquid to the needles at each pump operation. Thus, a fixed amount of liquid was dispensed out from each blunt needle tip, leading to the simultaneous or non-simultaneous ejection of two equal-sized droplets with minimum oscillation. The impact process of these droplets on a substrate was recorded with high-speed shadowgraphic imaging.

Experiments were carried out with distilled water ($\sigma = 0.073\ \mathrm{N\ m^{-1}}, \mu = 0.001$ mPa s and $\rho = 1000\ \mathrm{Kg\ m^{-3}}$) droplets and a smooth acrylic impact substrate (Perspex plate, $R_a \approx 1.17\ \mathrm{nm}$). Two high-speed cameras (Photron, FASTCAM APX RS and FASTCAM SA1.1) were synchronised at 9000 fps to simultaneously capture the front- and side-views of the droplet pair impact with spatial resolutions of 0.03- and 0.04-mm per pixel, respectively. The test area was illuminated uniformly by using two diffuser-paired LED lamps. A reference coordinate system was considered on the impact surface, with its origin in the middle of the distance between the impacting droplets' centres (**Figure 2**). The experimental data were extracted by analysing the recorded images using several image processing routines in MATLAB. The initial droplet diameter (D_0), the dimensionless inter-droplet spacing ($\Delta x^* =$

$\Delta x/D_0$) and the impact Weber number (We) were kept constant at 3.10 ± 0.04 mm, 1.86 ± 0.03 and 103 ± 2 respectively.

It is noted that, for all impact cases (simultaneous or non-simultaneous) reported in this study, the mean values are estimated from at least three realisations for each experimental condition. With a temporal resolution of ~ 0.11 ms (corresponding to the imaging rate of 9000 fps), 'simultaneous droplet impacts' occur when both droplets touch the solid surface at the same imaging frame (shown in **Figure 1(b)**). Henceforth, for non-simultaneous impacts, the droplet that impacts the substrate first will be termed as 'first droplet' and the next one as 'second droplet'. The reference dimensionless time $\tau = 0$ corresponds to the time of the touchdown of the first droplet, as shown at the inset (i.e. magnified views) of **Figure 2**. Similar to the dimensionless time τ, the time lag between impacts is made dimensionless as $\Delta\tau = \Delta t V_0/D_0$.

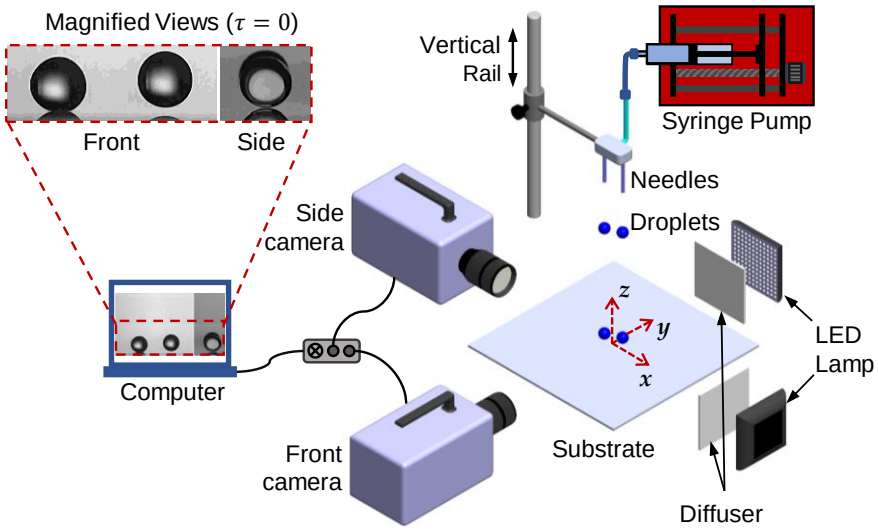

Figure 2. Schematic of the experimental setup. The test rig coordinate is set on the solid surface in the middle of the distance between the centres of the impacting droplets.

Results and Discussion

Figure 3 presents the droplet pair impact morphologies at different dimensionless times (τ) for both simultaneous ($\Delta\tau = 0$) and non-simultaneous impacts ($\Delta\tau$ ranges from 0 to 0.82), with a fixed inter-droplet spacing $\Delta x^* = 1.86 \pm 0.03$ and Weber number $We = 103 \pm 2$. For convenience and brevity, the image at the first row of each case corresponds to the time $\tau = \Delta\tau$, where the dimensionless time lag ($\Delta\tau$) between droplet impacts is different for individual cases. For the simultaneous impacts ($\Delta\tau = 0$), owing to the interaction of the spreading lamellas, a central sheet appears in the middle of two impacting droplets, which ascends vertically up to a certain time, and then gradually falls back on the surface, remaining vertical. The inset images, placed in the front-view images, reveal the instantaneous shape (side-view) of the central sheet (**Figure 3**). It is revealed that the central sheet ascends vertically with a rim-bounded regular two-dimensional (2D) 'semilunar' shape and, subsequently, instability cusps appear along the sheet rim as it descends towards the substrate. For non-simultaneous impacts ($\Delta\tau > 0$), the morphologies of the central sheet evolution differ depending on the time lag between impacts. For $\Delta\tau = 0.22$ and $\Delta\tau = 0.4$, the corresponding uprising central sheets appear to incline from the vertical axis (z-axis) towards the first droplet, unlike the vertical sheet for the simultaneous impacts. This sheet inclination

occurs due to the inequality of the momentum of the interacting lamellas, resulting from the non-simultaneous impacts of the droplets. The inclination angle of the sheet and the subsequent cusp instabilities at the sheet rim seem to increase with increasing $\Delta\tau$ from 0.22 to 0.4. However, these uprising sheets retain the 2D 'semilunar' shape (revealed in the inset images) with a roughly linear sheet base like that observed for the simultaneous impacts (**Figure 3**).

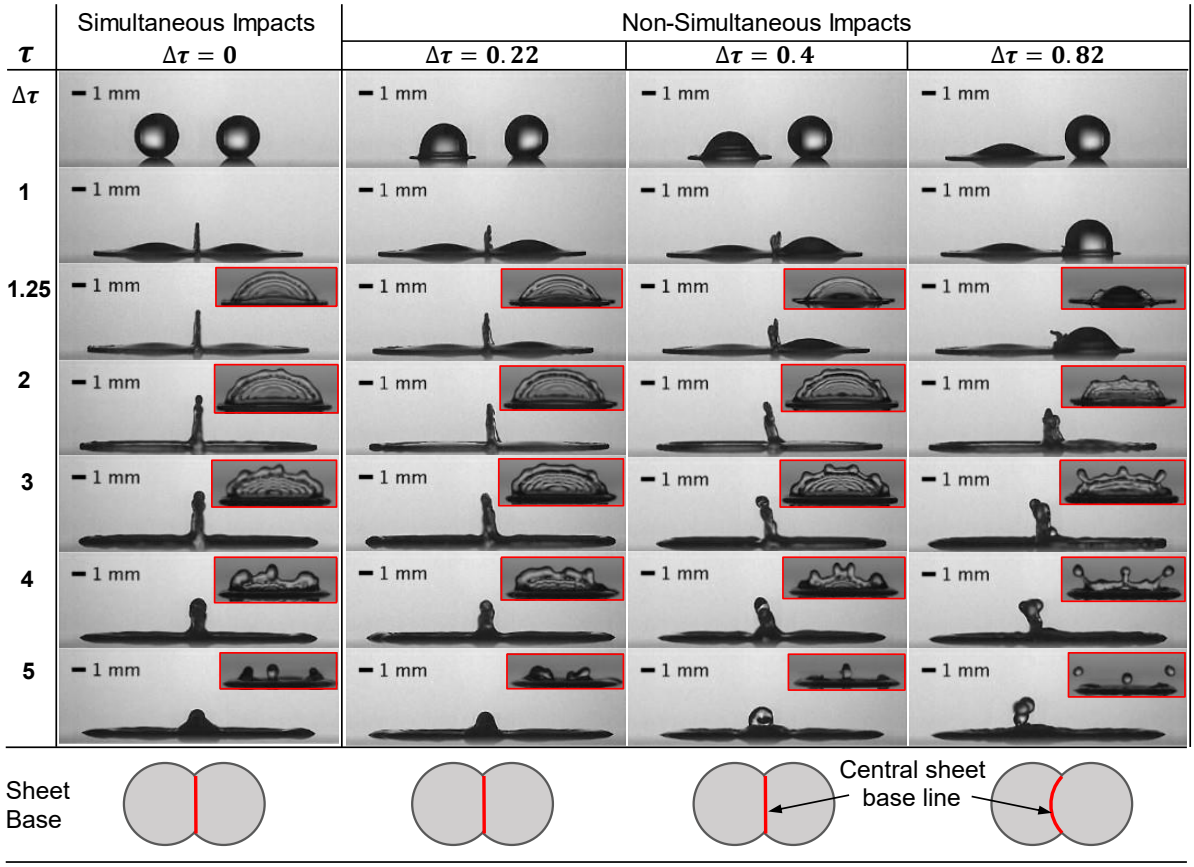

Figure 3. The effect of time lag ($\Delta\tau = \Delta t V_0/D_0$) between droplet impacts on the resulting impact morphologies. The scale bar in the front-view images is 1 mm. Inset images (not to scale) show the instantaneous shape (side-view) of the sheets. Simplified schematics of the base (linear or curved) of the uprising sheet are shown at the bottom of each case.

It is evident that, for the first three cases ($\Delta\tau = 0$, $\Delta\tau = 0.22$, and $\Delta\tau = 0.4$), the central sheets evolve due to the interaction of the outer lamella region of the droplets, namely lamella-lamella interaction. On the other hand, for $\Delta\tau = 0.82$, the time lag between impacts allows the spreading lamella of the first droplet to interact with the descending bulk liquid of the second droplet, namely lamella-droplet interaction. Consequently, a different shape of the uprising sheet evolves, namely a three-dimensional (3D) 'non-semilunar' sheet with a curved sheet base (**Figure 3**). Compared to all other cases, the cusps of this 3D sheet become more amplified during the retraction of this sheet, leading to finger-like jets and the subsequent breakup of the jets into secondary droplets (i.e. splashing).

Figure 4(a) shows the temporal evolution of the dimensionless vertical height of the central sheet ($H^*_{CS} = H_{CS}/D_0$), for four droplet pair impacts with different time lags ($\Delta\tau$) between impacts ranging from 0 to 0.4. In all these impact processes, the uprising sheet retains a 2D 'semilunar' shape, vertical or inclined, with a roughly linear sheet base. The error bars

represent the standard deviation from mean data, and the error bars are not visible where they are too small to exceed the size of the symbols. A higher $\Delta\tau$ delays the first instant of lamella-lamella interaction, and the maximum H^*_{CS} value decreases with increasing $\Delta\tau$. The maximum H^*_{CS} is $\sim 1.2D_0$ for $\Delta\tau = 0$, whereas it is $\sim 1.08D_0$ for $\Delta\tau = 0.4$. The inclination of the central sheet for the cases with $\Delta\tau > 0$ contributes to the reduction of the vertical height of the sheet. **Figure 4(b)** shows that the maximum value of the dimensionless central sheet width at its base, $W^*_{CS} = W_{CS}/D_0$, occurred later for a higher $\Delta\tau$. However, depending on $\Delta\tau$, the maximum W^*_{CS} does not vary significantly for these impact processes.

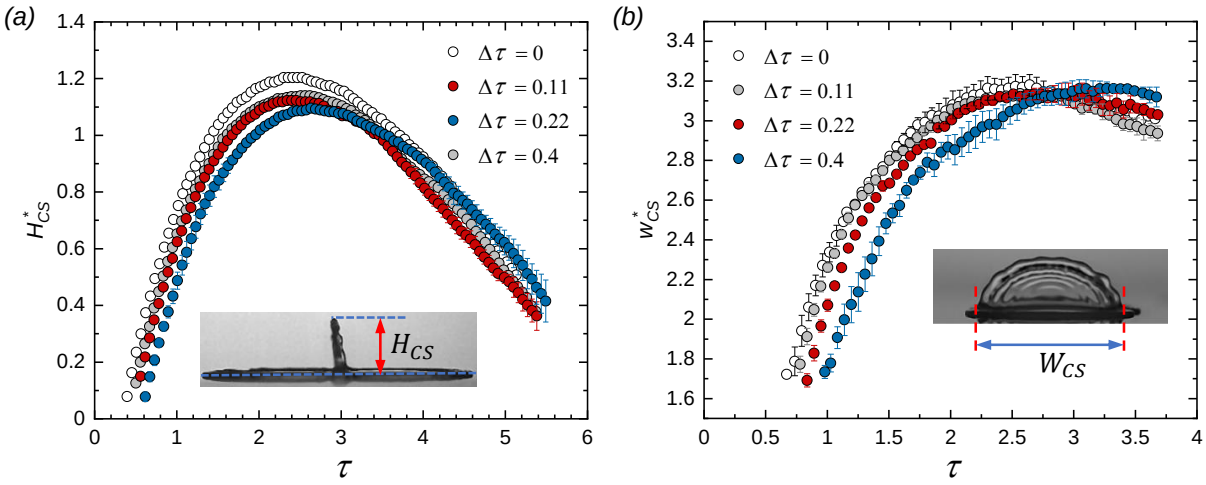

Figure 4. (a) Temporal variation of the dimensionless central sheet height ($H^*_{CS} = H_{CS}/D_0$) for different dimensionless time lags ($\Delta\tau$) between impacts. An error bar is the standard deviation around the mean. (b) Temporal variation of the dimensionless central sheet width ($W^*_{CS} = W_{CS}/D_0$) for different time lags. Inset images show the definition of H_{CS} and W_{CS}.

Figure 5(a) shows the temporal position of the central sheet base for the impact processes quantified in **Figure 4**. **Figure 5(a)** depicts the propagation of the lamella interaction line on the impact substrate. We define the position of the sheet base by a distance $d_{x,CS}$ (shown in **Figure 5(a)**) relative to the inter-droplet spacing Δx, i.e. by $d_{x,CS}/\Delta x$. To determine $d_{x,CS}$, an image analysis algorithm detects the middle point of the central sheet thickness along a horizontal line that is considered slightly above the surface to separate the sheet from the lamellas in the image (see the dashed yellow line in the right inset image of **Figure 5(a)**). It is noted that, as the thickness of the interacting lamella increases with τ, this separator line is shifted upwards in order to determine $d_{x,CS}$ for different batches of images. In **Figure 5(a)**, there are three possible positions for the central sheet: (i) in the middle between the two droplets' impact centres with $d_{x,CS}/\Delta x = 0$, (ii) closer to the first droplet with $d_{x,CS}/\Delta x < 0$, and (iii) closer to the second droplet with $d_{x,CS}/\Delta x > 0$. For $\Delta\tau = 0$, the central sheet initiates at $d_{x,CS}/\Delta x \approx 0$, remains close to this position throughout its evolution and eventually falls back on the surface at $d_{x,CS}/\Delta x \approx 0$, with minor deviations. Such temporal position of the central sheet agrees well with that for perfect simultaneous impacts of two identical droplets with exactly equal impacting velocities, where the sheet remains in the middle (i.e. $d_{x,CS}/\Delta x = 0$) throughout the sheet evolution [6]. On the other hand, with an increase in the time lag between impacts ($\Delta\tau = 0.11$ to 0.4), the central sheet initiates closer to the second droplet, and the position depends on $\Delta\tau$. For example, the initial $d_{x,CS}$ increases from

$\sim 0.025\Delta x$ to $\sim 0.12\Delta x$ as $\Delta\tau$ between impacts increases from 0.11 to 0.4. The change of the sheet position seems to be nearly invariant up to a certain time for each case, and, subsequently, the sheet gradually moves towards the first droplet before it falls back on the impact substrate. However, the overall shift of the central sheet position is not that significant relative to the inter-droplet spacing for these impact processes; the maximum is $0.14\Delta x$ for $\Delta\tau = 0.4$.

Figure 5(b) shows the temporal variation of the inclination angle (θ_{CS}) of the central sheet relative to the vertical z-axis. A positive θ_{CS} represents the sheet inclination towards the second droplet, whereas a negative θ_{CS} represents sheet inclination towards the first droplet (see the definition of θ_{CS} in the inset image). For simultaneous impacts ($\Delta\tau = 0$), the sheet remains vertical with $\theta_{CS} \approx 0°$, throughout its temporal evolution. For non-simultaneous cases ($\Delta\tau = 0.11$ to 0.4), the central sheet starts with an inclination towards the second droplet ($\theta_{CS} > 0°$), and with time τ, the sheet inclination shifts towards the first droplet (i.e. θ_{CS} becomes negative) during the ascent motion of the central sheet. In other words, the sheet inclination angle increases monotonically with the horizontal axis (x-axis) during its ascent motion. The inclination angle increases with increasing $\Delta\tau$, maximum for $\Delta\tau = 0.4$. For all cases, as the sheet starts to descend, it inclines back towards the z-axis again, i.e. the magnitude of θ_{CS} reduces again.

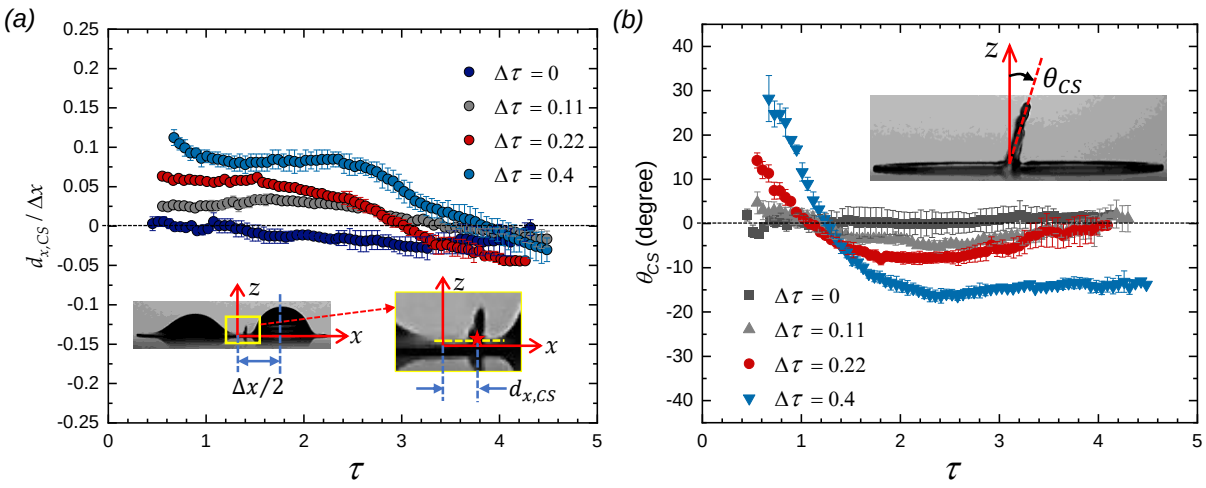

Figure 5. (a) Temporal variation of the dimensionless position of the central sheet base ($d_{x,CS}/\Delta x$) relative to the *z*-axis. (b) Temporal variation of the inclination angle of the central sheet (θ_{CS}) around the *z*-axis. An error bar is the standard deviation around the mean. Inset images show a schematic of the definition of the relevant parameters.

The central sheet inclination angle and the sheet movement primarily depend on the interplay of the momentum transfers from the interacting lamella fronts. The momentum transfer from a lamella front primarily depends on $T_L V_L^2$, where T_L is the average thickness of the lamella edge and V_L is the lamella edge velocity [10]. During the interaction of the two lamellas, the stagnating region along the interaction line redirects the lamella liquid flows upwardly and laterally, generating a central sheet. At the initial stage of this interaction, the first lamella front possesses a relatively higher T_L, whereas the second one possesses a relatively higher V_L. Therefore, the upwardly redirected thicker liquid from the first lamella tends to override that from the second one at this initial stage, leading to the central sheet inclination towards the second droplet. With time τ, the thickness of the second lamella

increases and becomes comparable with that of the first one, whilst V_L of the second lamella remains higher than that of the first lamella throughout the upward ascent of the central sheet. Therefore, the liquid flow from the second droplet starts to dominate over the first one, transforming the central sheet to vertical at some instance in time, which then inclines further towards the first droplet. After the initial violent collision and consequent flow redirection of the lamella liquid flows, the position of the central sheet does not vary appreciably during the initial ascent of the sheet. However, at later times, when the sheet height becomes significant the momentum difference increases at the sheet root and shifts it towards the first droplet. In addition, at later times, the lamella of the first droplet starts to recede earlier than the second one, which also contributes to the displacement of the central sheet root towards the first droplet.

The study reported, for the first time, the characteristics of the droplet interaction during droplet pair impacts on surfaces as a function of the time lag between droplet impacts and shows significant changes in the temporal evolution of the central sheet that is formed due to the droplet interaction. The effect of the time lag between the impact times of two droplets on a surface demonstrates the importance of the liquid flows dynamics and the consequences on the potential generation of new droplets after the impact, which can influence the relevant practical applications.

Conclusions

This study investigated the interaction of two identical droplets during their impact on a solid substrate simultaneously or non-simultaneously, with a particular focus on the evolution of the central sheet. For a given inter-droplet spacing and impact Weber number, the central sheet evolves perpendicular to the impact substrate with a two-dimensional (2D) ‘semilunar’ shape and linear base for simultaneous impacts. On the other hand, the morphologies of the central sheet temporal evolution vary for non-simultaneous impacts, depending on the time lag between the impacts. With an increase in the time lag, the sheet becomes inclined but retains the 2D ‘semilunar shape’ and linear base for lower time lags. The height, width, position, and angle of the sheet are time-dependent and governed by the interplay of the momentum transfer from the interacting lamellas to the central sheet. However, after a certain time lag, the central sheet is not inclined with a 2D shape but evolves with a 3D shape and curved base. A 3D sheet increases the probability of the generation of secondary droplets. All these morphological and quantitative characteristics of the present study provide fundamental insight into a ubiquitous yet too less studied multiple droplet impact dynamics.

Acknowledgements

The present study is supported by the Commonwealth Scholarship Commission in the UK.

Nomenclature

D_0	initial droplet diameter [m]
$d_{x,CS}$	distance of central sheet [m]
g	gravitational acceleration [ms^{-2}]
H_{CS}	height of the central sheet [m]
R_a	average surface roughness [m]
T_L	average thickness of lamella edge [m]
V_L	velocity of lamella front [ms^{-1}]
V_0	average velocity of impacting droplets [ms^{-2}]
Δx	inter-droplet spacing [m]

We Weber number [-]
$\Delta\tau$ dimensionless time lag between droplet impacts [-]
μ dynamic viscosity [Pas]
ρ density [kgm^{-3}]
σ surface tension [Nm^{-1}]
τ dimensionless time [-]
θ_{CS} inclination angle of the central sheet [°]

References

[1] Josserand, C., and Thoroddsen, S. T., 2016, "Drop Impact on a Solid Surface," Annu. Rev. Fluid Mech., **48**(1), pp. 365–391.
[2] Yarin, A. L., 2006, "Drop Impact Dynamics: Splashing, Spreading, Receding, Bouncing..," Annu. Rev. Fluid Mech., **38**, pp. 159–192.
[3] Benther, J. D., Pelaez-Restrepo, J. D., Stanley, C., and Rosengarten, G., 2021, "Heat Transfer during Multiple Droplet Impingement and Spray Cooling: Review and Prospects for Enhanced Surfaces," Int. J. Heat Mass Transf., **178**, p. 121587.
[4] Cossali, G. E., Marengo, M., and Santini, M., 2007, "Splashing Characteristics of Multiple and Single Drop Impacts onto a Thin Liquid Film," 6th Int. Conf. Multiph. Flow, (835).
[5] Barnes, H. A., Hardalupas, Y., Taylor, A. M. K. P., and Wilkins, J. H., 1999, "An Investigation of the Interaction between Two Adjacent Impinging Droplets.," *ILASS Europe 1999*, pp. 1–7.
[6] Roisman, I. V, Prunet-Foch, B., Tropea, C., and Vignes-Adler, M., 2002, "Multiple Drop Impact onto a Dry Solid Substrate," J. Colloid Interface Sci., **256**(2), pp. 396–410.
[7] Gultekin, A., Erkan, N., Ozdemir, E., Colak, U., and Suzuki, S., 2021, "Simultaneous Multiple Droplet Impact and Their Interactions on a Heated Surface," Exp. Therm. Fluid Sci., **120**(September 2020), p. 110255.
[8] Liang, G., Yu, H., Chen, L., and Shen, S., 2019, "Interfacial Phenomena in Impact of Droplet Array on Solid Wall," Acta Mech.
[9] Ersoy, N. E., and Eslamian, M., 2020, "Central Uprising Sheet in Simultaneous and Near-Simultaneous Impact of Two High Kinetic Energy Droplets onto Dry Surface and Thin Liquid Film," Phys. Fluids, **32**(1).
[10] Wang, Y., and Bourouiba, L., 2018, "Non-Isolated Drop Impact on Surfaces," J. Fluid Mech., **835**, pp. 24–44.